Sans-Tresserras, JÁ.; Manjón, FJ.; Popescu, C.; Muñoz, A.; Rodríguez-Hernández, P.; Jordá, JL.; Rey Garcia, F. (2016). Arsenolite: a quasi-hydrostatic solid pressure transmitting medium. Journal of Physics: Condensed Matter. 28(47):475403-1-475403-7. doi:10.1088/0953-8984/28/47/475403.

Arsenolite: a quasi-hydrostatic solid pressure transmitting medium

J.A. Sans,[1,*] F.J. Manjón,[1] C. Popescu,[2] A. Muñoz,[3] P. Rodríguez-Hernández,[3] J.L. Jordá,[4] and F. Rey[4]

[1] Instituto de Diseño para la Fabricación y Producción Automatizada, Universidad Politécnica de Valencia, 46022 Valencia (Spain)

[2] CELLS-ALBA Synchrotron Light Facility, 08290 Cerdanyola, Barcelona (Spain)

[3] Departamento de Física, Instituto de Materiales y Nanotecnología, Universidad de La Laguna, 38205, La Laguna, Spain

[4] Instituto de Tecnología Química (UPV-CSIC), Universidad Politécnica de Valencia, Consejo Superior de Investigaciones Científicas. 46022 Valencia (Spain)

Abstract. This study reports the experimental characterization of the hydrostatic properties of arsenolite (As_4O_6), a molecular solid which is one of the softest minerals in absence of hydrogen bonding. The high compressibility of arsenolite and its stability up to 15 GPa have been proved by x-ray diffraction measurements and the progressive loss of hydrostaticity with increasing pressure up to 20 GPa has been monitored by the ruby photoluminescence. Arsenolite has been found to exhibit a hydrostatic behavior up to 2.5 GPa and a quasi-hydrostatic behavior up to 10 GPa at room temperature. This result opens the way to explore other molecular solids as possible quasi-hydrostatic pressure-transmitting media. The validity of arsenolite as an insulating, stable, non-penetrating and quasi-hydrostatic medium is explored by the study of the x-ray diffraction of zeolite ITQ-29 at high pressure.

I. Introduction

Pressure is a primary thermodynamic variable that allows tuning the material properties in a large range. Therefore, high-pressure experiments are important tools which help us to understand the properties of matter both at ambient and extreme conditions. Application of pressure to materials induces a great reduction of interatomic distances, which intensifies interatomic interactions; hence it allows the study of material properties in a broader range than by changing temperature, its thermodynamic

* Corresponding author. E-mail address: juasant2@upv.es
Tel.: + 34 96 387 52 69, Fax: + 34 96 387 71 49

parameter counterpart. Besides, high-pressure techniques are also extensively used to synthesize compounds with different crystalline structures and properties without variation of their chemical stoichiometry and to synthesize new and unexpected compounds **[1]**.

The diverse high-pressure devices, experimental techniques and materials with different properties makes difficult to find the optimal conditions to obtain reliable results. Amongst all these conditions, the choice of the medium which transmits the pressure from the instrument to the compressed sample is extremely important. In most cases, the only requirement for this medium is to be a hydrostatic pressure-transmitting medium (PTM) according to Pascal's principle; i.e., a compound that allows the homogeneous application of pressure to the sample without directional or shear stress in its structure. In fact, the loss of hydrostatic conditions leads to uniaxial distortions which affect the compressibility of the structure and could derive in non-rigorous results, which could make difficult their comparison with purely hydrostatic theoretical predictions **[2]**.

The choice of an optimal PTM is based on the pressure range, the technique employed, and the material studied in a particular case, but the easiness to manipulate it and the difficulty of the loading procedure should also be considered. In pressure ranges above 10 GPa, the use of gas PTMs such as argon **[3,4]**, neon **[3,5]** or helium **[6,7]** is preferred to assure a wider hydrostatic range **[8]**. However, the lack of reactivity and the wide range of hydrostaticity of noble gases contrast with the difficulty to manipulate them and the specific equipment required for the loading procedure. In fact, the use of these gases is limited to diamond anvil cells (DACs) and is barely applied for transport properties, except in temperature dependent measurements.

On the other hand, in pressure ranges below 10 GPa, liquid fluids such as silicone oil **[9,10]**, FC84-FC87 Fluorinert mixture **[11]**, Daphne 7474 **[12]**, (16:3:1) methanol-ethanol-water **[4]**, or (4:1) methanol-ethanol mixture **[4]** are extensively used as PTMs due to their good hydrostatic behavior at low pressures and the easiness of loading in a DAC. The transparency of these PTMs in the visible region makes them ideal for spectroscopic studies in the UV-visible range, x-ray diffraction and low-frequency Raman scattering measurements. However, they have Raman peaks at high frequencies and exhibit a very high infrared response (due to vibrational properties of their characteristic carbon-hydrogen, carbon-oxide and hydrogen-oxide bonds) **[13]**.

Consequently, transparent solid PTMs, like KBr, although exhibiting a strong non-hydrostatic behavior above 6 GPa **[14]**, are preferred for infrared measurements and Raman measurements in the high-frequency region.

Some types of materials and techniques require solid PTM for studies of materials under compression. Regarding materials, the study of open-framework structures, such as zeolites, need the use of solid PTM since fluids could penetrate into the different porous cavities of the structure yielding to unexpected results in comparison with the case in which the PTM does not penetrate into the pores. Regarding techniques, transport measurements at high-pressures usually require the use of an insulating and non-magnetic solid PTM so that a good electrical insulation between the studied sample and the electric contacts with the gasket (and also from metallic anvils in the case of using a large volume press) is ensured. For that purpose, some insulating solid compounds like NaCl **[15]**, hexagonal-BN **[16]**, Na **[17]** and epoxy **[18]** are exploited. The main drawback of these solid PTMs is that they exhibit a rather non-hydrostatic behavior at room temperature.

Arsenolite (As_2O_3 indeed As_4O_6) is the cubic polymorph of arsenic oxide [space group 227, *Fd-3m*, Z=16], whose hardness is intermediate between that of Talc ($Mg_3Si_4O_{11}\cdot H_2O$) and Gypsum ($CaSO_4\cdot 2H_2O$); being these two minerals the softest materials in the Moss scale. This compound is a molecular solid with an open framework structure composed of discrete As_4O_6 molecular units, exhibiting strong covalent interatomic As-O bonds, which are linked by weak van der Waals forces in order to form a 3D solid structure. In particular, the structure of the As_4O_6 molecular cage can be described by the overlap of four pseudo–tetrahedral units consisting of an As atom surrounded by three O ligands and a cationic lone electron pair (LEP) in such a way that they form a ball with all cation and anion LEPs pointing towards the external part of the cage. Unlike other arsenic oxide polymorphs, pseudo-tetrahedra in arsenolite are configured in closed-compact adamantane-type As_4O_6 molecular cages bonded together thanks to weak van der Waals forces (see **Fig. 1**). Among the properties of arsenolite, we can mention its strong chemical stability and lack of reactivity (it is an oxide mineral obtained by oxidation of As-rich ore deposits as arsenic sulfide or by hydrolysis of arsenic chloride) **[19]** and that it is an insulating material with a bandgap above 4 eV at room pressure and above 3 eV up to 15 GPa **[20,21]**. Additionally, the

solubility of arsenolite has been fully characterized by a number of studies **[22,23]** showing a slow dynamics to reach the equilibrium conditions.

In this work, we will analyse the compressibility of arsenolite, its range of hydrostaticity, and how arsenolite can be applied to a case study, such as a zeolite, in order to show that arsenolite is an insulating solid compound, easy to manipulate, with a strong compressibility, high chemical inertness, and structural stability up to 15 GPa, which is a good candidate as a quasi-hydrostatic PTM up to 10 GPa in measurements of structural and electrical properties under pressure. We will show that arsenolite is a better solid PTM than CsI, KBr, NaCl, and h-BN so it could substitute these solid PTMs in high-pressure experiments. The main drawback of arsenolite is its toxicity, but this could be easily overcome by handling it with gloves and mask, a common equipment in high-pressure laboratories.

II. Method

Highly pure arsenolite (As_4O_6) powder (99.999%) has been commercially obtained from Sigma Aldrich Company. Two high-pressure angle-dispersive x-ray diffraction (ADXRD) experiments at room temperature have been conducted in a membrane-type DAC. In the first experiment, we have studied the equation of state (EoS) of arsenolite **[19]** using as PTM either a 4:1 methanol-ethanol mixture or silicone oil, but also without any PTM. Pressure inside the DAC was calibrated through the EoS of copper **[24]**. In the second one, we have studied the structural evolution of zeolite ITQ-29 under compression using arsenolite as a PTM. In this latter experiment, the EoS of copper **[24]** and arsenolite **[19]** were used as a pressure callibrants. A good agreement has been obtained in the estimation of the pressure by both materials. Both ADXRD experiments have been performed at the BL04-MSPD beamline **[25]** of ALBA synchrotron with an incident monochromatic wavelength of 0.4246 Å focused to 20 x 20 μm with a pinhole of 50 μm to cut the x-ray beam tail. Images have been collected using a SX165 CCD detector. One-dimensional diffraction profiles of intensity as a function of 2θ have been obtained by integration of the observed 2-dimensional diffraction patterns with the Fit2D software **[26]**.

Additionally, we have carried out two photoluminescence (PL) experiments. In the first one, we have measured the PL of a 5 μm-size ruby, which was placed into the

center of the cavity pressure at room temperature using arsenolite as a PTM. In the second one, we have measured the PL of four ruby chips of similar dimensions randomly distributed from the center to the edge of the pressure cavity. This last experiment has allowed us to determine the standard deviation of the pressure estimation along the cavity. Both PL measurements have been performed with a Horiba Jobin Yvon LabRAM HR-UV microspectrometer equipped with a thermoelectric-cooled multi-channel CCD detector and with a spectral resolution below 2 cm^{-1}. A HeNe laser (632.8 nm line) has been used to excite the ruby photoluminescence **[27]**. No detectable influence of the laser radiation on the temperature of the illuminated ruby chip has been found.

III. Results and discussions

In a previous work, we reported the structural characterization of compressed arsenolite by means of ADXRD measurements under compression using different PTMs **[19]**. It was reported that a similar EoS of arsenolite was obtained using non-penetrating PTMs, but a completely different result was obtained when He is used as a PTM due to its inclusion into the arsenolite's crystalline structure **[19,20]**. In particular, non-penetrating PTM gave rise to a bulk modulus of B_0=7(1) GPa, which is in good agreement (see **Fig. 2**) with our theoretical calculations **[19]** (B_0=7.6 GPa). It must be stressed that arsenolite's bulk modulus is much lower than those reported for commonly used solid PTM, such as CsI **[28]** (B_0=13.0 GPa), KBr **[29]** (B_0=14.4 GPa), NaCl **[30]** (B_0=25.03(8) GPa), and h-BN **[31]** (B_0=29.1(4) GPa).

It is well known that hydrostatic conditions are closely determined not only by the bulk modulus but also by the shear modulus, which does not imply a volume change. Our theoretically simulated elastic properties of arsenolite **[19]** yield a shear modulus of 9.3 GPa at ambient conditions, which is of the order of that found in CsI (6.2-8.7 GPa) **[28]** and lower than the values reported for KBr **[32]** (14.8 GPa) and NaCl **[33]** (14.9 GPa). Unfortunately, we cannot give a value for the shear modulus of h-BN due to the lack of experimental measurements and the large discrepancy of theoretical values found in the literature, which was already exposed by Ooi and co-workers **[34]**. In spite of this lack of information on h-BN, we can suggest a value for

the shear modulus of h-BN around 15 GPa on the basis of the strong relationship between bulk and shear moduli found in similar compounds.

The remarkably small bulk and shear moduli of arsenolite here reported are given by the extraordinary compressibility of the intermolecular distances between As_4O_6 molecular cages (see **Fig. 1**). The presence of cation and anion LEPs is responsible for the formation of the molecular cages and the weak van der Waals interactions that bond them. Whereas these molecular units remain almost unalterable with increasing pressure due to the small reduction of intramolecular distances, the intermolecular distance between the different cages is rapidly reduced below 10 GPa due to the strong compressibility of the cationic LEP; i.e., the LEP activity progressively decreases with increasing pressure as observed in a number of group-15 related compounds **[35]**. The strong compression of intermolecular distances results in a strong increase of intermolecular interactions. These interactions are proposed to trigger the instability of molecular cages leading to a pressure-induced amorphization (PIA) of arsenolite as observed in previous studies **[36,19]**. In particular, arsenolite compressed without any PTM gives rise to the appearance of PIA above 10 GPa.

In order to explore the hydrostatic regime of arsenolite under pressure, we have analyzed the stress caused in ruby chips randomly distributed along the gasketed pressure cavity and surrounded by As_4O_6 **[37]**. For that purpose, we have conducted PL measurements of the peaks R_1 and R_2 of ruby (Cr-doped Al_2O_3), which correspond to internal transitions of the Cr^{3+} ion in corundum aluminum oxide. In particular, R_1 and R_2 lines are assigned to transitions to the $^4A_2$ ground state from the $2\bar{A}$ and $\bar{E}$ states (originated from the degeneracy break of the ^2E excited state), respectively **[38-43]**. The application of pressure causes an increase of the trigonal crystal-field strength, which induces a change in the transition energy of both lines **[44]**. Besides, the crystal-field strength depends strongly on directionality, which makes this parameter very sensitive to shear stress. The evolution of the R_1-R_2 splitting should remain nearly constant with pressure as long as hydrostatic conditions are satisfied, but the splitting increases once the pressure applied is not homogeneous.

The analysis of the R_1 and R_2 peaks serves to study the effect of the hydrostaticity in ruby **[44]**; however, the evolution of the FWHM of both peaks under pressure can be also used as a method to determine the pressure gradients and local shear stresses **[45]**. Piermarini et al. reported the broadening of the R_1 peak with the

solidification of several liquid PTMs and suggested the distribution of several rubies along the pressure cavity in order to determine the standard deviation of the pressure calculated from each one, as the optimal method to obtain accurately the hydrostatic range of the medium **[45]**. Later, Klotz et al. **[8]** used this method to determine the hydrostatic range of 11 PTMs. In most cases, both methods were found to be equivalent and gave rise to similar results. In fluid PTMs, the determination of the critical pressure at which the medium solidifies and loses the hydrostatic behavior strongly depends on the position of the ruby **[8]**. For this reason, the last method suits perfectly to the study of fluid PTMs, but it gives similar results to the former in the case of solid PTMs. Here, we report the hydrostatic range of arsenolite by both methods, analyzing the PL lines of a ruby chip under pressure and estimating the standard deviation of the pressure calculated from rubies randomly distributed along the pressure cavity.

For the first method, we inserted a ruby chip into the center of a pressure cavity. **Figure 3** shows the peaks corresponding to the optical emission lines R_1 and R_2 of this ruby. A fit of these peaks to a Voigt-shape function (Lorentzian profile convoluted with a Gaussian function), which takes into account the resolution of the spectroscopic system given by the Gaussian convolution, allowed us to extract the amplitude, central wavelength, and full-width half maximum (FWHM) of the Lorentzian peaks. The R_1-R_2 splitting shows a typical monotonous decrease up to 4-5 GPa, which is characteristic of a hydrostatic behavior under pressure (**Fig. 3b top**). Above this pressure, we can observe a progressive non-linear increase of this parameter with pressure, which is more marked above 10 GPa. These features have been associated to the presence of deviatoric stresses in the ruby chip **[44]**. This result is confirmed by the increase of the FWHM (**Fig. 3b down**) of the R_1 peak above 4 GPa, being this progressive broadening more abrupt from 10 GPa.

Arsenolite's results can be compared with those of other solid PTMs. For instance, a progressive broadening of the R_1 peaks is observed at very low pressures in NaCl **[46]**, so we can conclude that NaCl does not behave as a hydrostatic PTM even at ambient pressure. On the other hand, KBr shows deviatoric stresses in their structure when it transits from B1 to B2 phase above 2.1 GPa **[14]**. Moreover, the hydrostatic range here reported for arsenolite is better than some typical liquid PTMs such as Fluorinert mixture **[8]** (hydrostatic up to 2 GPa) and comparable to Daphne 7474 **[12,8]** (hydrostatic up to 4 GPa), iso-n-pentane (hydrostatic up to 5-6 GPa) and silicone oil **[8]**

(hydrostatic up to 4-8 GPa). However, its range of hydrostatic behavior is lower than that of methanol-ethanol mixtures **[8]** (hydrostatic up to 10.5 GPa for 16:3:1 methanol-ethanol-water and 4:1 methanol-ethanol mixture).

For the second method, we have randomly distributed four ruby chips from the center to the border of the gasketted pressure cavity, as it is shown in the inset of **Figure 4**. The distance between the rubies is estimated from the size of the pressure cavity to be roughly 40 microns. This method shows that the hydrostatic range exhibited by arsenolite is very limited since the standard deviation (**Figure 4**) is less than 0.1 GPa below 2.5 GPa. This means that arsenolite exhibits a similar behavior as the mixture 1:1 FC84-FC87 Fluorinert where the hydrostatic range extends to 2.3 GPa **[8]**. It is noteworthy to expose that the value of the standard deviation shows a small value in the high pressure regime (~0.6 GPa at 20 GPa), which is competitive with those obtained in liquids. For instance, at 20 GPa, the standard deviation for different liquids are: ~2 GPa for 4:1 methanol-ethanol and 16:3:1 methanol-ethanol-water mixture and ~2.2 GPa for silicone oil. **Figure 5** shows the analysis of the stress produced in the most centered and remote ruby (named ruby1 and ruby4, respectively), which reveals a similar behavior below 10 GPa. In both rubies, the R1-R2 peak distance decreases up to 10 GPa and then increases. However, this difference increases more rapidly for ruby4 than for ruby1, thus indicating that the latter is more stressed. The pressure dependence of the FWHM corresponding to the PL of the R1 peak for both rubies yields similar results, as shown in **Figure 5**. These findings corroborate the quasi-hydrostatic behavior observed in the standard deviation, with values smaller than 0.3 GPa up to 10 GPa.

Finally, the good properties of arsenolite as a PTM have been corroborated by analyzing the structural evolution of zeolite ITQ-29 under compression **[47]**. This compound has an open framework structure with cavities of different sizes, so the use of fluid PTM, which might penetrate any of these cavities, must be avoided in studies of this material under compression. Besides, this compound is quite sensitive to non-hydrostatic conditions due to its molecular structure. Uniaxial distortions could easily induce structural deformations, which can be the onset of a phase transition. In this regard, the structural behavior of zeolite ITQ-29 with pressure was already reported using silicone oil as a PTM and two phase transitions were observed **[48]**. The cubic symmetry of arsenolite gives rise to few Bragg diffraction peaks reducing the possibility to overlap with the sample pattern. A fully reversible one at 1.2 GPa and a non-

reversible one around 3.2 GPa which leads to the obtaining of the novel zeolite ITQ-50 at ambient conditions. **Fig. 6** displays the evolution of the ADXRD patterns of zeolite ITQ-29 under compression using arsenolite as a PTM. As observed, our experiment shows a similar behavior as the one previously reported using silicone oil **[48]**. Between 0.9 and 1.9 GPa, there is a distortion of the cubic structure of ITQ-29, which is consistent with the transition pressure of 1.2 GPa already reported. Similarly, the irreversible phase transition is completed between 2.7 and 3.7 GPa in our experiment, which is consistent with the transition pressure of 3.2 GPa already reported. Therefore, the good agreement between the results obtained in this experiment and the previous one using silicon oil validate the use of arsenolite as a non-penetrating quasi-hydrostatic PTM.

IV. Conclusions

We have shown that arsenolite, the cubic polymorph of arsenic oxide, is a solid insulating compound, easy to manipulate, with very low bulk and shear moduli, high chemical inertness, and structural stability up to 15 GPa, which shows a good hydrostatic range for a solid compound (up to 2.5 GPa) at room temperature. Therefore, we propose arsenolite as a good candidate for a quasi-hydrostatic PTM up to 10 GPa at room temperature in measurements of electrical properties under pressure and for high-pressure structural studies of porous compounds and materials with open-framework structures in order to avoid penetration of the PTM inside their cavities. Additionally, this work paves the way to explore other molecular solids as possible quasi-hydrostatic PTM.

ACKNOWLEDGMENTS

This work has been performed under financial support from Spanish MINECO under projects MAT2013-46649-C4-2/3-P and MAT2015-71070-REDC. JAS acknowledges “Juan de la Cierva” fellowship program for financial support. We also thank D. Calatayud, J. J. García, T. M. Godoy, A. Zapata, and A. Cuenca for fruitful discussions. Authors thank ALBA light source for beam allocation at beamline MSPD. JLJ and FR acknowledge financial support through SEV-2012-0267, ERC-ADG-2014-

671903, Consolider Ingenio 2010-Multicat (CSD-2009-0050) and MAT2012-38567-C02-01 projects.

References:

[1] R. J. Hemley, and N. W. Ashcroft, Phys. Today 51, 26 (1998).

[2] A. Mujica, Angel Rubio, A. Muñoz, and R. J. Needs, Rev. Mod. Phys. 75, 863 (2003).

[3] P. M. Bell, and H. K. Mao. Carnegie Institution of Washington Year Book vol **80**, 404 (1981).

[4] R. J. Angel, M. Bujak, J. Zhao, G. D. Gatta, and S. D. Jacobsen. J. Appl. Cryst. **40**, 26 (2007).

[5] Y. Meng, D. J. Weidner, and Y. Fei. Geophys. Res. Lett. **20**, 1147 (1993).

[6] K. Takemura, and A. Dewaele. Phys. Rev. B **78**, 104119 (2008).

[7] A. Dewaele, and P. Loubeyre. High Press. Res. **27**, 419 (2007).

[8] S. Klotz, J.-C. Chervin, P. Munsch, and G. Le Marchand. J. Phys. D: Appl. Phys. **42**, 075413 (2009).

[9] D. D. Ragan, D. R. Clark, and D. Schiferl. Rev. Sci. Instrum.**67**, 494 (1996).

[10] Y. Shen, R. S. Kumar, M. Pravia and M. F. Nicol. Rev. Sci. Instrum. **75**, 4450 (2004).

[11] V. A. Sidorov, and R. A. Sadykov. J. Phys.: Condens. Matter. **17**, S3005 (2005).

[12] K. Murata, K. Yokogawa, H. Yoshino, S. Klotz, P. Munsch, A. Irizawa, M. Nishiyama, K. Lizuka, T. Nanba, T. Okada, Y. Shiraga, and S. Aoyama. Rev. Sci. Inst. **79**, 085101 (2008).

[13] C. R. Howle, C. J. Homer, R. J. Hopkins, and J. P. Reid. Phys. Chem. Chem. Phys. **9**, 5344 (2007).

[14] J. Zhao and N. L. Ross. J. Phys.: Condens. Matter **27**, 185402 (2015).

[15] C. Meade and R. Jeanloz. J. Geophys. Res. **93**, 3270 (1988).

[16] P. Piszora, W. Nowicki, J. Darul, and C. Lathe. Synchrotron Radiation in Natural Science **9**, 145 (2010).

[17] M. Hanfland, K. Syassen, and J. Köhler. J. Appl. Phys. **91**, 4143 (2002).

[18] A. K. Singh and G. C. Kennedy. J. Appl. Phys. **48**, 3362 (1977).

[19] Handbook of Preparative Inorganic Chemistry, 2nd Ed. Edited by G. Brauer, Academic Press, 1963, NY.

[20] J. A. Sans, F. J. Manjón, C. Popescu, V. P. Cuenca-Gotor, O. Gomis, A. Muñoz, P. Rodríguez-Hernández, J. Contreras-García, J. Pellicer-Porres, A. L. J. Pereira, D. Santamaría-Pérez, and A. Segura. Phys. Rev. B **93**, 054102 (2016).

[21] P. A. Gunka, K. F. Dziubek, A. Gładysiak, M. Dranka, J. Piechota, M. Hanfland, A. Katrusiak, and J. Zachara. Cryst. Growth Des. **15**, 374 (2015).

[22] G.S. Pokrovski, J.-M. Bény, and A. V. Zotov. J. Solut. Chem. **28**, 1307 (1999).

[23] D. K. Nordstrom, J. Majzlan, and E. Königsberger. Rev. Min. Geochem. **79**, 217 (2014).

[24] A. Dewaele, P. Loubeyre, M. Mezouar. Phys. Rev. B **70**, 094112 (2004).

[25] F. Fauth, I. Peral, C. Popescu, M. Knapp, Powder. Diffr. **28**, S360 (2013).

[26] A.P. Hammersley, S.O. Svensson, M. Hanfland, A.N. Fitch, D. Hausermann. High Press. Res. **14**, 235 (1996).

[27] B. Garcia-Domene, H. M. Ortiz, O. Gomis, J. A. Sans, F. J. Manjón, A. Muñoz, P. Rodríguez-Hernández, S. N. Achary, D. Errandonea, D. Martínez-García, A. H. Romero, A. Singhal, and A. K. Tyagi. J. Appl. Phys. **112**, 123511 (2012).

[28] R. M. Ribeiro, J. Coutinho, V. J. B. Torres, R. Jones, S. J. Sque, S. Öberg, M. J. Shaw and P. R. Briddon, Ab initio study of CsI and its surface, Phys. Rev. B 74, 035430 (2006).

[29] R. W. Roberts, and C. S. Smith. J. Phys. Chem. Solids **31**, 619 (1970).

[30] D. L. Decker. J. Appl. Phys. **42**, 3239 (1971).

[31] K. Fuchizaki, T. Nakamichi, H. Saitoh, and Y. Katayama. Solid State Comm. **148**, 390 (2008).

[32] V. P. Matsokin, and G. A. Petchenko. Low Temp. Phys. **26**, 517 (2000).

[33] A. E. Gleason. Elasticity of Materials at High Pressure. UC Berkeley: Earth & Planetary Science (2010).

[34] N. Ooi, V. Rajan, J. Gottlieb, Y. Catherine, and J. B. Adams. Modelling Simul. Mater. Sci. Eng. **14**, 515 (2006).

[35] A. L. J. Pereira, J. A. Sans, R. Vilaplana, O. Gomis, F. J. Manjón, P. Rodríguez-Hernández, A. Muñoz, C. Popescu, and A. Beltrán. J. Phys. Chem. C **118**, 23189 (2014).

[36] A. Grzechnik. J. Sol. State Chem. **144**, 416 (1999).

[37] J. C. Chervin, B. Canny and M. Mancinelli. High Pressure Res. **21,** 305 (2001)

[38] S. Sugano andY. Tanabe. J. Phys. Soc. Jpn. **13**, 880 (1958).

[39] S. Sugano and I. Tsujikawa. J. Phys. Soc. Jpn. **13**, 899 (1958).

[40] A.L. Schawlow, D.L.Wood, andA.M. Clogston. Phys. Rev. Lett. **3**, 271 (1959).
[41] D.S. McClure. Electronic spectra of molecules and ions in crystals part II, spectra of ions in crystals, in Solid State Physics Vol. 9, F. Seitz and D. Turnbull, eds., Academic Press, NewYork, 1959, 399–524.
[42] R.A. Ford, Spectrochim. Acta **16**, 582 (1960).
[43] W. Low. J. Chem. Phys. **33**, 1162 (1960).
[44] K. Syassen. High Press. Res. **28**, 75 (2008).
[45] G. J. Piermarini, S. Block, and J. D. Barnett. J. Appl. Phys. **44**, 5377 (1973).
[46] N. Tateiwa and Y. Haga. Rev. Sci. Inst. **80**, 123901 (2009).
[47] A. Corma, F. Rey, J. Rius, M. J. Sabater, S. Valencia. Nature **431**, 287 (2004).
[48] J. L. Jordá, F. Rey, G. Sastre, S. Valencia, M. Palomino, A. Corma, A. Segura, D. Errandonea, R. Lacomba, F. J. Manjón, O. Gomis, A. K. Kleppe, A. P. Jephcoat, M. Amboage, and J. A. Rodríguez-Velamazán. Angewandte Chemie Int. Ed. **52**, 10458 (2013).

Figure captions

Figure 1. Detailed scheme of the unit cell of arsenolite (As_4O_6)

Figure 2. EoS of compressed arsenolite measured using experimental ethanol-methanol mixture (blue points), silicone oil (red points) and without PTM (black points). EoS fit to a 3rd order Birch-Murnaghan equation is plotted with dashed lines and the evolution of the theoretically simulated structure of compressed arsenolite is plotted with a solid line.

Figure 3. (a) PL spectra of R_1 and R_2 peaks of compressed ruby. They are vertically shifted for the sake of clearness. (b:top) Evolution of the R_1-R_2 peak splitting with increasing pressure for a ruby chip surrounded by arsenolite inside a DAC and (b:down) Idem for the FWHM of the R_1 peak.

Figure 4. Pressure dependence of the standard deviation (σ) calculated using arsenolite as PTM. Inset shows the distribution of ruby chips along the pressure cavity.

Figure 5. Evolution of the R_1-R_2 peak splitting and FWHM of the R_1 peak with increasing pressure for (a) ruby1 and (b) ruby4.

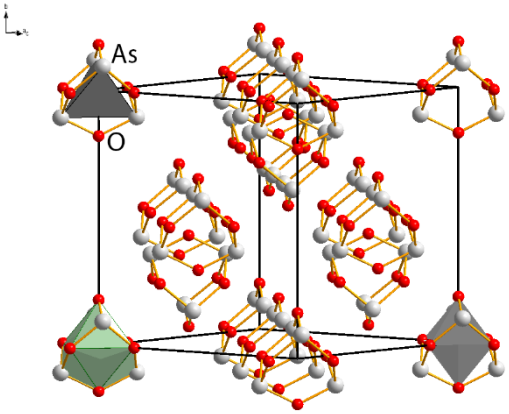

Figure 6. ADXRD patterns of ITQ-29 zeolite using arsenolite as PTM inside a DAC. Asterisks indicate the new peaks appearing in the different transitions already reported. They are vertically shifted for the sake of clearness. The pattern of the recovered sample after pressure release is also shown to evidence the irreversibility of the second phase transition.

Figure 1

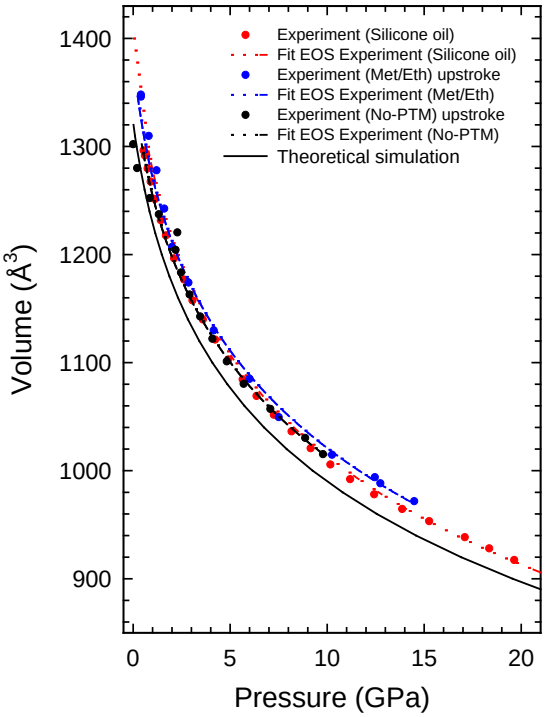
Experiment (Silicone oil)
Fit EOS Experiment (Silicone oil)
Experiment (Met/Eth) upstroke
Fit EOS Experiment (Met/Eth)
Experiment (No-PTM) upstroke
Fit EOS Experiment (No-PTM)
Theoretical simulation
Volume (Å3)
Pressure (GPa)
1400
1300
1200
1100
1000
900
0
5
10
15
20

Figure 2

Figure 3

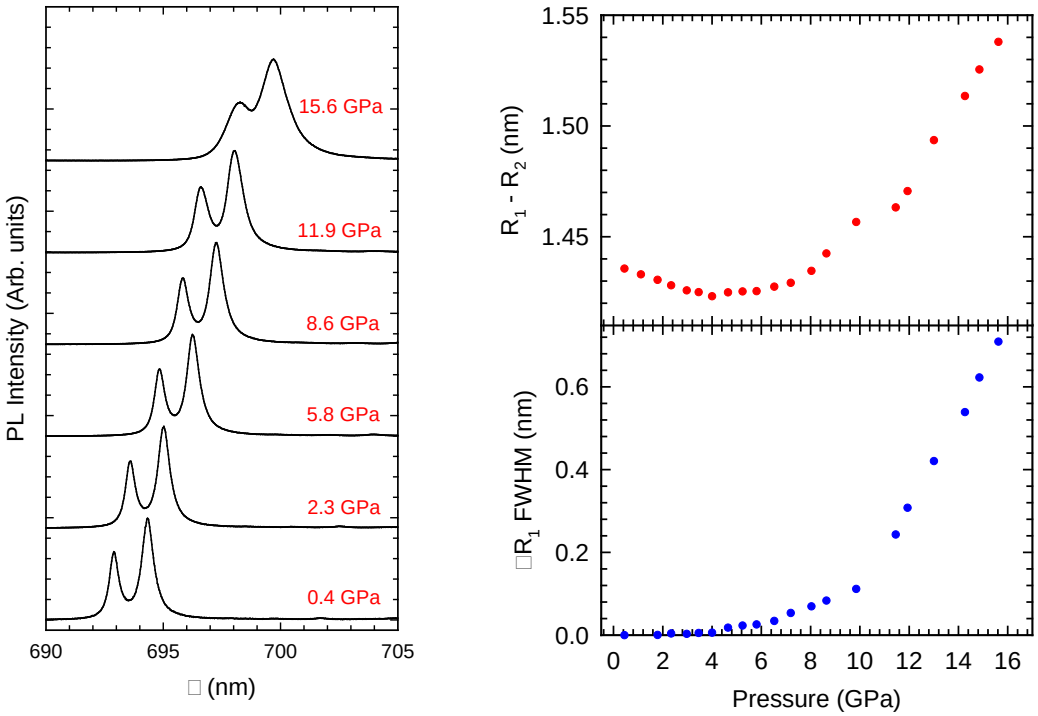
15.6 GPa
11.9 GPa
8.6 GPa
5.8 GPa
2.3 GPa
0.4 GPa
PL Intensity (Arb. units)
690
695
700
705
(nm)
1.55
1.50
1.45
R1 - R2 (nm)
0.6
0.4
0.2
0.0
R1 FWHM (nm)
0
2
4
6
8
10
12
14
16
Pressure (GPa)

Figure 4

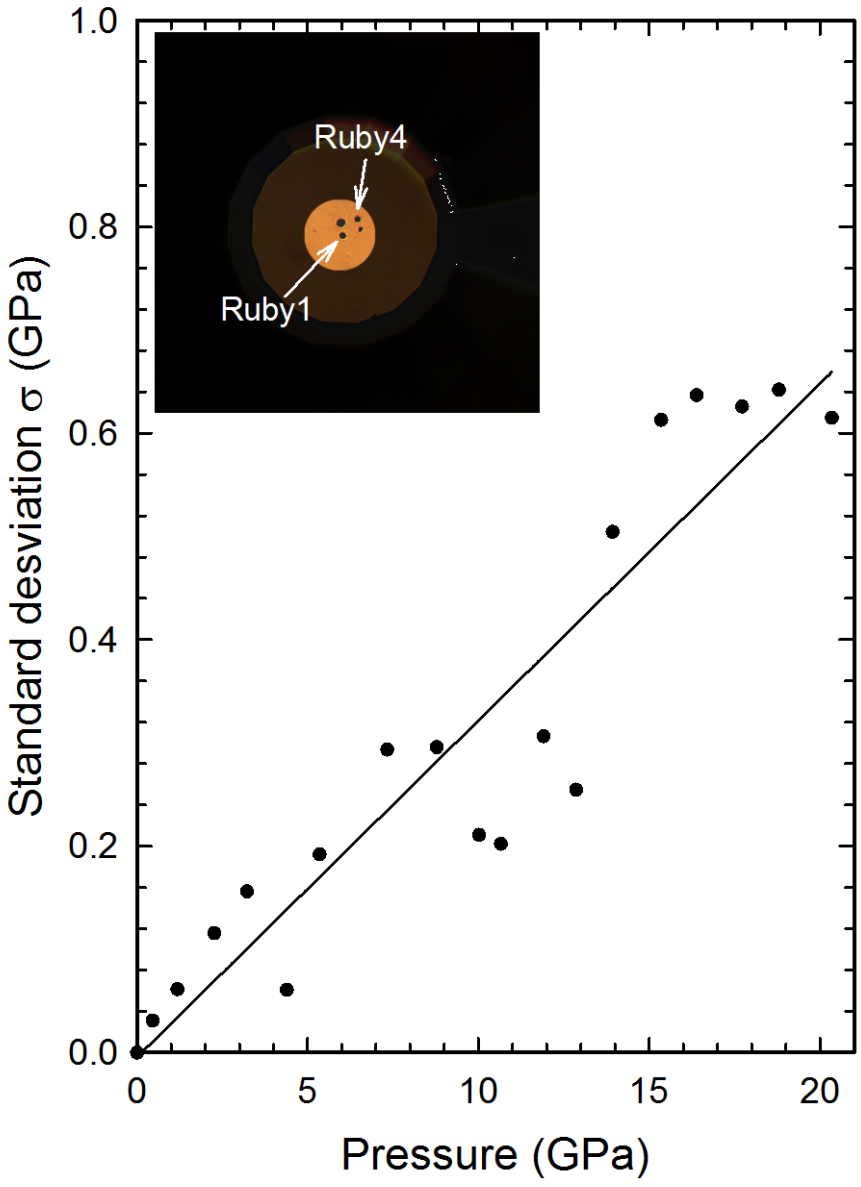
Ruby4
Ruby1
Standard desviation σ (GPa)
Pressure (GPa)
0.0
0.2
0.4
0.6
0.8
1.0
0
5
10
15
20

Figure 5

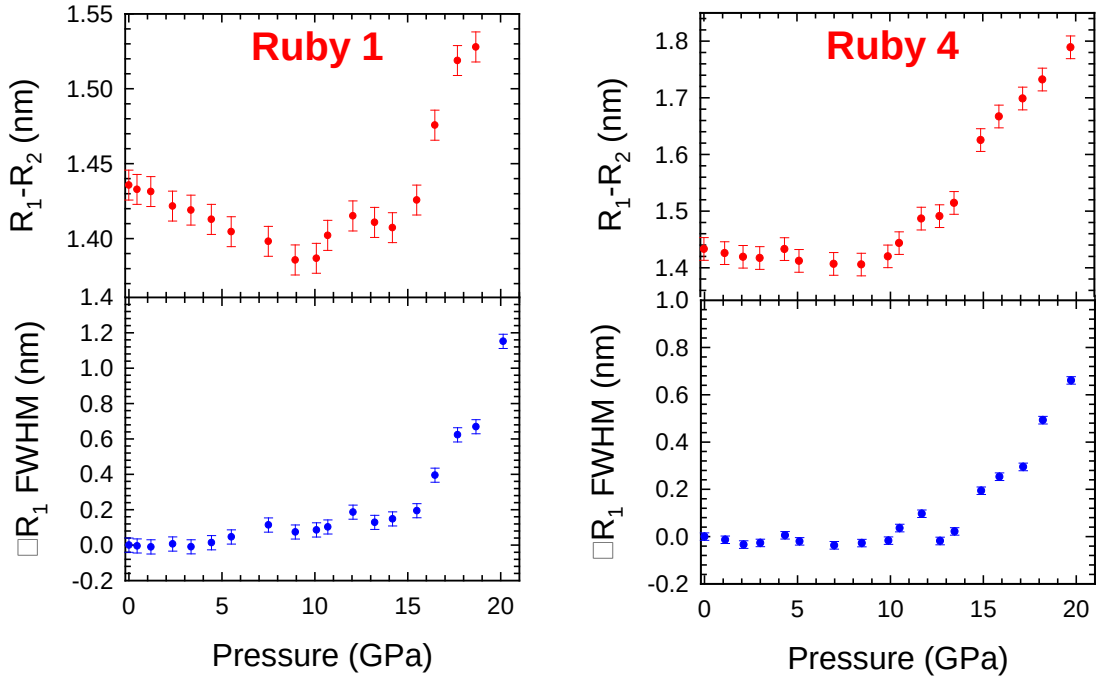
Ruby 1
Ruby 4
R1-R2 (nm)
R1 FWHM (nm)
Pressure (GPa)
1.55
1.50
1.45
1.40
1.4
1.2
1.0
0.8
0.6
0.4
0.2
0.0
-0.2
0
5
10
15
20
1.8
1.7
1.6
1.5
1.4
1.0

Figure 6

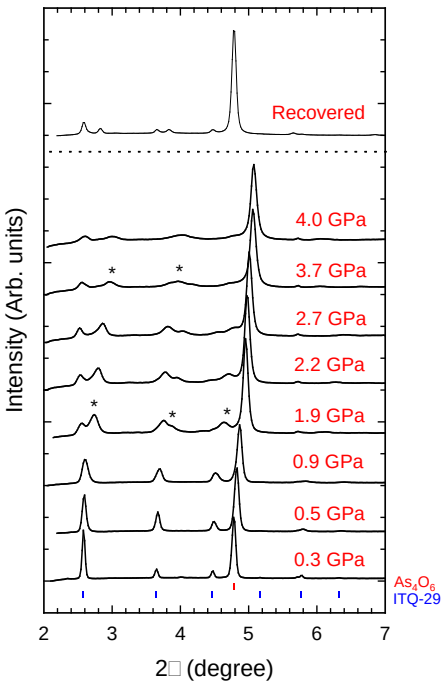
Recovered
4.0 GPa
3.7 GPa
2.7 GPa
2.2 GPa
1.9 GPa
0.9 GPa
0.5 GPa
0.3 GPa
*
As4O6
ITQ-29
Intensity (Arb. units)
2
3
4
5
6
7
2□ (degree)